Influence of roughness distributions and correlations on x-ray diffraction from superlattices

A. P. Payne and B. M. Clemens

Department of Materials Science and Engineering, Stanford University, Stanford, California 94305-2205

(Received 11 May 1992; revised manuscript received 17 August 1992)

Interfacial roughness in superlattices is currently a topic of significant interest as a result of its impact on device applications and its influence on thin-film phenomena. In this work we examine the effects of interfacial roughness on x-ray diffraction from superlattices. By means of a Taylor expansion of the amplitude reflection coefficient of the multilayer, we present general expressions for the specular, diffuse, and total diffracted intensity from a rough multilayer and examine how these quantities are influenced by roughness distributions and correlations among the interfaces. We present analytical solutions for exemplary structures including superlattices with no roughness, correlated roughness, uncorrelated roughness, and partially correlated roughness. We also present a model for cumulative roughening in multilayers and characterize its diffraction signature. We show how specific configurations of interfacial roughness give rise to a variety of additional features in diffraction spectra beyond the customary pseudo-Debye-Waller attenuation. Specifically, we illustrate how roughness *distributions* induce broadening of the diffraction features, and how modulations in the diffuse scattering result directly from interfacial roughness *correlations*. We also show that partial correlation of interfacial roughness constitutes a second important source of peak broadening.

I. INTRODUCTION

X-ray diffraction has been used extensively as a rapid, nondestructive means of eliciting structural information from superlattices. The technique can be applied to a wide range of structural phenomena including strain,[1,2] epitaxial orientation,[3,4] growth morphology,[5,6] interfacial mixing and amorphization,[7,8] and crystalline coherency.[9,10] An important aspect of multilayer structure receiving much attention recently is the roughness of the interfaces. From a technological standpoint, interfacial roughness in multilayers is important in a variety of applications. Roughness is extremely important, for example, in multilayer optical elements for x-ray wavelengths, as it dramatically affects the reflectivity of these structures.[11] Although currently debated, recent experimental studies on coupled magnetic multilayers exhibiting giant magnetoresistance indicate that interface roughness enhances the effect.[12] Because of the increased presence of multilayer structures in technological applications, the ability to measure and control interface roughness will presumably become more critical. Thus an understanding of the x-ray-diffraction (XRD) signature of interfacial roughness is crucial to the development of XRD as a useful analytical technique.

X-ray diffraction from superlattices can be divided into two regimes. These regimes are commonly referred to as "low angle" and "high angle," though they more generally correspond to size regimes of the scattering vector q. The low-q regime is defined by $|q| \approx 2\pi/\Lambda$ while the high-q regime is given by $|q| \approx 2\pi/d$, where Λ is the artificially induced bilayer period and d is the average interatomic spacing perpendicular to the scattering vector. Features in the high-q superlattice spectra result from interference between scattering from atomic periodicity

and the artificial periodicity imposed by the superlattice structure. These features are highly sensitive to atomic structure at the interface and can, for instance, be used to determine whether crystalline registry is preserved across interfaces.[13,14] Features in the low-q spectra, on the other hand, result exclusively from the imposed layer structure, and are sensitive to morphological features of the interface such as roughness. Several reports describe the extraction of interface roughness parameters from experimental diffraction spectra.[15,16]

Since diffraction experiments measure intensity rather than electric field, direct access to the structure of the superlattice through Fourier transformation is generally precluded by the lack of phase information. For this reason, structural information from superlattices is typically extracted by fitting spectra generated from models to the experimental data. In the high-q regime, scattering is weak and kinematic[17] models are typically employed. Nonidealities such as interfacial alloying,[18] discrete and continuous layer thickness fluctuations,[13,19] finite coherence lengths,[9] and epitaxial strains[20] have been incorporated. Though kinematic models are often used in the low-q regime, this approach is not valid in the presence of strong dynamical scattering. In this case, dynamical diffraction models[21] or optical models[22] are more appropriate. The effects of interface roughness (layer thickness fluctuations) on low-q scattering have been recognized and incorporated in several models,[20] and several theoretical treatments for scattering in rough multilayers have been presented, including those by Green's functions[23,24] and first-order perturbation theory.[25,26] The effects of roughness distributions and correlations on diffraction for superlattices has not been explicitly treated, however, and this is the subject of the present work.

One of the most common approaches for treating

roughness in multilayers is to fit the specular θ-2θ diffraction spectra to recursive Fresnel models using the Born approximation to treat interfacial roughness.[27,28] This treatment leads to a pseudo-Debye-Waller attenuation of the diffracted intensity, $\exp\{-q_z^2 n_0^2 \sigma^2\}$,[29–31] where σ is the rms interface roughness of the layers and n_0 is the index of refraction of the environment. While attenuation of the superlattice peaks is invariably observed in real superlattices, this treatment does not account for other changes to the ideal spectrum caused by interface roughness. Furthermore, analysis of interface roughness solely through the specular reflectivity is limited in that it cannot differentiate surface roughness from interdiffusion.[31] Differentiating these effects is essentially a problem of measuring the lateral length scale of the roughness, which can be done through careful measurement of diffusely scattered intensity along nonspecular directions.[15] The diffusely diffracted spectrum can also reveal unique information regarding the vertical correlation of roughness within the superlattice. Although it is well known that multilayers exhibit peaks in the specular scattering at the Bragg condition ($q_z = m2\pi/\Lambda$) whose amplitudes are determined by the Fourier coefficients of the composition modulation,[17] a perhaps lesser known fact is that nonideal multilayers can exhibit similar peaks in the diffuse scattering.[33] Though the nature of this enhancement is debated,[34] it is generally recognized that enhanced diffuse scattering is related to interfacial defects which are to some degree replicated or *correlated* from interface to interface within the multilayer.[26]

In the low-q regime, the diffraction spectrum is composed of specular and diffuse components, both of which are strong functions of q and σ. Despite this, many diffraction models treat either the total diffracted intensity[20] or the specular intensity,[35] though neither is explicitly measured in a typical diffraction experiment. In the θ-2θ diffraction geometry, one measures the specular intensity plus the portion of the diffuse intensity scattered in the specular direction. Before one can properly account for this in a diffraction model, it is necessary to calculate both the specular and diffuse components of the scattered radiation. In this work, we will develop general expressions for the specular, diffuse, and total diffracted intensity from nonideal multilayers exhibiting roughness distributions and correlations. We will define precisely what we mean by the terms "specular," "diffuse," "distri-bution," and "correlation," and will treat the cases schematized in Fig. 1 which are, in order of increasing complexity, (a) no roughness, (b) correlated roughness, (c) uncorrelated roughness, and (d) partially correlated roughness. Finally, we will present a model for structural evolution in multilayers under non-equilibrium growth conditions and discuss its diffraction signature in terms of cumulative roughness distributions and correlations. Through this simple set of models we present a rigorous yet intuitive means of assessing the influence of interfacial roughness on superlattice diffraction.

II. SCATTERING IN ROUGH MULTILAYERS

A. Rough surfaces and random Gaussian variables

We will describe a rough surface in terms of a random Gaussian variable z defined as the deviation of the interface from its mean position, an approach which has been successfully applied to scattering from rough surfaces.[31,32] The functional form of z is given by the interface profile function $z(x)$, illustrated in Fig. 2(a). Each interface profile function varies about a local origin positioned at the mean interface location within the superlattice. The probability that a point on the interface is located between a value z and $z + dz$ is described by $P(z)$, the Gaussian probability density distribution.

$$P(z) = \frac{1}{\sqrt{2\pi}\sigma}\exp\left[-\frac{z^2}{2\sigma^2}\right] . \tag{1}$$

The magnitude of the rms roughness is given by σ, the width of this distribution as shown in Fig. 2(b). We will frequently evaluate the expectation value of a function [i.e., $\langle \mathcal{F}(z) \rangle$], mathematically given by Eq. (2) below:

$$\langle \mathcal{F}(z) \rangle = \int_{-\infty}^{+\infty} \mathcal{F}(z)P(z)dz . \tag{2}$$

Frequently, the arguments in $\mathcal{F}$ involve a complex exponential dependence on the interface profile function $z(x)$, resulting in expectation values which assume the following form:

$$\langle \exp[i\kappa z(x)] \rangle = \exp(-\kappa^2\sigma^2/2) , \tag{3}$$

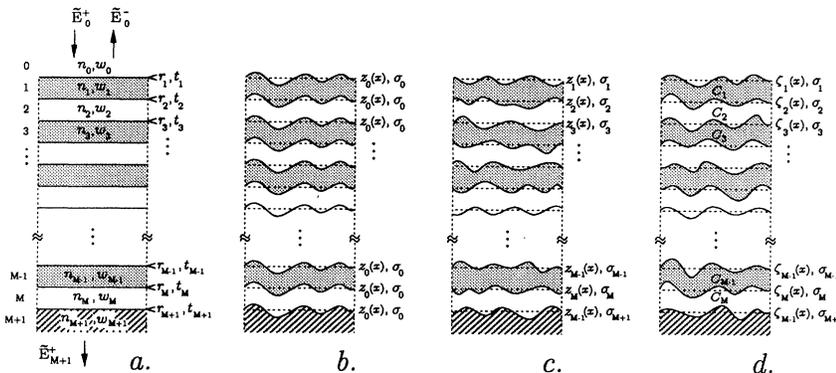where κ is the wave vector magnitude ($\kappa = 2\pi/\lambda$) and λ is

FIG. 1. Schematics of the nonideal multilayer structures treated in this work: (a) no roughness, (b) correlated roughness, (c) uncorrelated roughness, and (d) partially correlated roughness. Each interface and the layer directly underneath it are assigned the same index, j. Quantities associated with interfaces $(r,t,z(x),\zeta(x),\sigma)$ are shown to the right of the interface, while those associated with layer (n,w,C) are shown inside the layer. Note that the numbering scheme for the layering is from top to bottom of the multilayer. Incident, reflected, and transmitted electromagnetic waves are shown for the first case.
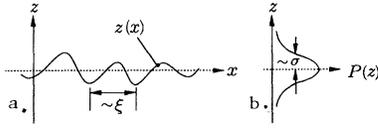
FIG. 2. The rough interface is described by the interface profile function $z(x)$ shown in (a) which varies with Gaussian statistics about the mean position of the interface, $z \equiv 0$. The rms amplitude of the roughness is described by the standard deviation σ of the Gaussian probability density distribution $P(z)$ shown in (b). The lateral coherence length of the roughness, ξ, is approximated by the distance between surface asperities and is assumed to be much smaller than the rms roughness ($\sigma \ll \xi$).

the x-ray wavelength. A related quantity is the magnitude of the scattering vector, $|\mathbf{q}|$, which, for *specular* scattering, is given by $q_z = |\mathbf{q}| = 4\pi \sin\theta / \lambda$. For normal incidence, the wave vector is related to the scattering vector by $\kappa = q_z / 2$.

B. Interfacial roughness correlations

It is important to distinguish two types of correlation in the multilayer structure. The "correlation length" of the roughness, ξ, typically refers to the lateral distance along an interface at which the z heights of two points on the surface become statistically uncorrelated.[32] This dimension is approximated by the lateral distance between surface asperities in a rough interface as shown in Fig. 2(a). Another type of correlation, treated in this work, refers to how the profiles of consecutive interfaces map onto one another in a multilayer. Some authors distinguish this as "z correlation."[15] If two interfaces are completely correlated, their interface profile function will be equal [Fig. 1(b)]. For completely uncorrelated interfaces, the interface profile functions will be distinct and statistically uncorrelated [Fig. 1(c)]. The degree of correlation of interfaces bounding the jth layer can be described by the correlation coefficient C_j,

$$C_j = \frac{\langle z_j(x) z_{j+1}(x) \rangle}{[\langle z_j(x)^2 \rangle \langle z_{j+1}(x)^2 \rangle]^{1/2}} \, . \tag{4}$$

It is also useful to define the deviation coefficient D_j, defined such that $C_j^2 + D_j^2 = 1$. For total correlation $C = 1$ and $D = 0$ while for no correlation $C = 0$ and $D = 1$. Partially correlated interfaces are characterized by fractional values for C and D [Fig. 1(d)]. These interfaces can be described by decomposing the interface profile functions into correlated and uncorrelated components, as will be described in Sec. IV D.

C. Variance of a rough surface

The variance V of a random variable describes the spread of that variable about its mean value. The variance of a rough surface is given by

$$V[z(x)] = \langle [z(x) - \langle z(x) \rangle]^2 \rangle = \langle z(x)^2 \rangle - \langle z(x) \rangle^2 \, . \tag{5}$$

Since we define the origin of the function to lie at the local mean interface position, $\langle z(x) \rangle \equiv 0$, the variance becomes simply the square of the rms roughness of the interface profile function: $V = \langle z(x)^2 \rangle = \sigma^2$. The variance of a rough surface is extremely important in determining its scattering properties. This is because a nonzero variance for the surface profile function will induce a nonzero variance in the amplitude reflection coefficient ρ, leading to diffuse scattering. This will be developed in the following section.

D. Specular and diffuse scattering

The amplitude reflection coefficient ρ is in general a complex quantity. The variance of a complex expression can nevertheless be calculated in a manner similar to that in Eq. (5):

$$V(\rho) = \langle |\rho - \langle \rho \rangle|^2 \rangle = \langle \rho \rho^* \rangle - \langle \rho \rangle \langle \rho^* \rangle \, . \tag{6}$$

By means of Eq. (6), one is able to partition the total reflected intensity (R) into total, specular, and diffuse components given below.[31] The subscripts t, s, and d refer to total, specular, and diffuse, respectively, while ρ is the amplitude reflection coefficient of the scattering. Similar equations can be derived for the transmitted intensity (T), by replacing ρ by τ, the amplitude transmission coefficient, in Eqs. (7)–(9) below,

$$R_t = \langle \rho \rho^* \rangle \, , \tag{7}$$

$$R_s = \langle \rho \rangle \langle \rho^* \rangle \, , \tag{8}$$

$$R_d = \langle \rho \rho^* \rangle - \langle \rho \rangle \langle \rho^* \rangle \, . \tag{9}$$

Figure 3 shows a general case of scattering from a surface. The scattering vector $\mathbf{q}$ is defined by the incident and scattered x rays, $\mathbf{S_0}$ and $\mathbf{S}$ according to $\mathbf{q} = \kappa(\mathbf{S} - \mathbf{S_0})$. Specular scattering is associated with equality of the incidence and reflection angles θ_i and θ_o, whereupon the scattering vector assumes the form $\mathbf{q} = (0, 0, q_z)$. In nonspecular scattering, these angles are not equal and $\mathbf{q} = (q_x, q_y, q_z)$ as shown in the figure. Though the terms "nonspecular" and "diffuse" are often used interchangeably, this is misleading since it implies that there is no diffuse scattering in the specular direction. Diffuse
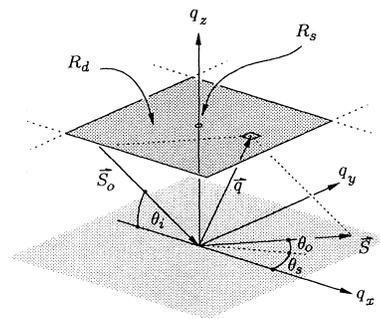

FIG. 3. Diagram showing a generalized scattering event in reciprocal space. Since $\theta_i \neq \theta_o$, the depicted scattering is nonspecular. The integrated diffuse intensity R_d is contained in the (q_x, q_y) plane, while the specular intensity R_s is concentrated at the local origin of the plane, $(0, 0, q_z)$.

scattering can occur into any direction above the sample surface, including the specular direction. A better interpretation of specular and diffuse scattering is that diffuse scattering is the field scattered by the *deviation* of interface from that of a smooth multilayer, whereas specular scattering results from the *average* change in electron density associated with traversing the interface. The spatial breadth of the distribution of scattered intensity from a surface is thus directly related to the width of the surface height distribution, σ.

An implicit caveat of the above treatment is that R_d refers strictly to the *integrated* diffuse intensity over the 2π steradians over the surface. In reciprocal space, R_d corresponds to the integrated intensity over the q_x, q_y plane at a particular value of q_z, as illustrated in Fig. 3. The intensity at $(0, 0, q_z)$ is determined by the specular reflectivity R_s, in addition to the diffuse intensity associated with this point. R_d describes the total intensity apportioned to the diffuse field but not how that intensity is spatially distributed within the diffuse field. This distribution depends on both the magnitude of the roughness, σ, and on its in-plane spatial frequency distribution, approximated by coherence length ξ. This is an active area of experimental[15,34,36] and theoretical[32,37,38] research.

E. Wave propagation in a rough multilayer

Following the approach of Eastman,[25] the scattering from a rough multilayer can be described in terms of a phase perturbation to waves traveling through the film. Figure 4 shows an interface described by the interface profile function $z_j(x)$, which separates two media of different refractive indices, n_{j-1} and n_j. Vectors $\tilde{E}_{j-1}^{+}$, $\tilde{E}_{j-1}^{-}$, and $\tilde{E}_j^{+}$ are the normally incident, reflected, and transmitted waves, respectively, reflected and transmitted components, respectively, while $\tilde{E}_j^{-}$ is the incident wave from underlying layers. The phase of a wave traveling through this interface will be shifted from that of a wave passing through a smooth interface on account of the
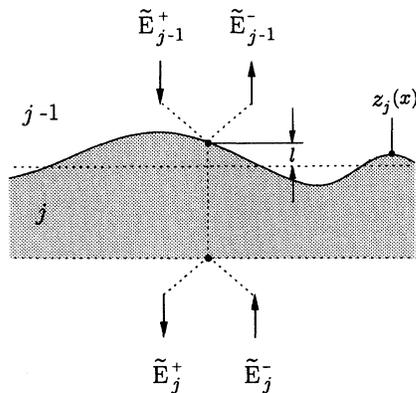

FIG. 4. Schematic showing how roughness is treated in the phase perturbation model. Horizontal field components are equated at the interface after compensating for the phase difference caused by displacement of the interface by the distance l.

propagation through extra path length $l = z_j(x)$. In the case of a superlattice each layer and associated interface can be described by a transfer matrix S_j which relates the four interacting electromagnetic waves:

$$\begin{bmatrix} \tilde{E}_{j-1}^{+} \\ \tilde{E}_{j-1}^{-} \end{bmatrix} = S_j \begin{bmatrix} \tilde{E}_j^{+} \\ \tilde{E}_j^{-} \end{bmatrix}, \tag{10}$$

where S_j is given by

$$S_j = \frac{1}{t_j} \begin{bmatrix} \exp(ia_j) & r_j\exp(ib_j) \\ r_j\exp(-ib_j) & \exp(-ia_j) \end{bmatrix}. \tag{11}$$

Here, r_j and t_j are the Fresnel amplitude reflection and transmission coefficients for an ideal interface at normal incidence:

$$r_j = \frac{n_{j-1} - n_j}{n_{j-1} + n_j}, \tag{12}$$

$$t_j = \frac{2n_{j-1}}{n_{j-1} + n_j}. \tag{13}$$

The quantities a and b are abbreviations of the following quantities:

$$a_j = \kappa \Delta_j z_j(x) + \phi_j, \tag{14}$$

$$b_j = \kappa \Sigma_j z_j(x) - \phi_j^*. \tag{15}$$

Following the notation used by Eastman,[25] Σ_j and Δ_j are shorthand notations for the sum and difference of the refractive indices of materials separated by the jth interface:

$$\Sigma_j = n_{j-1} + n_j, \tag{16}$$

$$\Delta_j = n_{j-1} - n_j. \tag{17}$$

In addition, ϕ_j is the phase factor associated with transversing a layer of average thickness w_j and refractive index n_j at normal incidence: $\phi_j = \kappa n_j w_j$. The transfer matrix for the entire multilayer is simply the product of the individual transfer matrices for each layer:

$$Z = S_1 S_2 S_3 \cdots S_{M-1} S_M S_{M+1}. \tag{18}$$

Since there is no back-reflected wave incident from the bottom of the multilayer, $\tilde{E}_j^{-} = 0$, and the amplitude reflection coefficient of the entire superlattice, ρ, is determined by a ratio of matrix elements:

$$\rho = \tilde{E}_0^{-} / \tilde{E}_0^{+} = Z_{21} / Z_{11}. \tag{19}$$

The phase perturbation approach assumes there is no large difference between the *horizontal* and tangential field components at the interface, and also neglects local changes in the angle of incidence induced by the roughness. Both assumptions are valid assuming that the interface profile function is everywhere differentiable and that the amplitude of the roughness is small compared with its lateral length scale ($\sigma \ll \xi$).[39] Numerous experiments show that the condition $\sigma \ll \xi$ is often fulfilled for multilayers prepared on smooth substrates.[36]

F. Scattering from a single rough interface

It is instructive to compare the scattering from rough multilayers with that from a single rough interface. For this reason, we now apply the formalism developed above to a single rough interface. We let $j = 1$ such that the interface bounds materials with refractive indices n_0 and n_1. The interface roughness is σ_1. By making the appropriate substitutions in Eqs. (10)–(19), we find that

$$\rho = \widetilde{E}_0^- / \widetilde{E}_0^+ = r_1 \exp[-2i\kappa n_0 z_1(x)] \ . \tag{20}$$

By substituting this amplitude reflection coefficient into Eqs. (7)–(9) and evaluating the expectation values using Eq. (3), we produce the well-known results for the total, specular, and diffuse components of the reflected intensity from the rough surface[31] given below. It is evident that while the roughness has no effect on the total reflected intensity, it does induce an exponential modulation of the specular and diffuse fields according to the pseudo-Debye-Waller damping term $\exp\{-4\kappa^2 n_0^2 \sigma_0^2\}$.

$$R_t = r_1^2 \ , \tag{21}$$

$$R_s = r_1^2 \exp(-4\kappa^2 n_0^2 \sigma_1^2) \ , \tag{22}$$

$$R_d = r_1^2 [1 - \exp(-4\kappa^2 n_0^2 \sigma_1^2)] \ . \tag{23}$$

III. APPROXIMATIONS

A. Taylor expansion of multilayer reflectivity

In calculating the reflected intensity from rough multilayers, it is clear from Eqs. (19) and (7)–(9) that expectation values involving rational arguments must be evaluated. For some of the cases treated here this is inconsequential, while for others it is a severe impediment. For the case of perfectly correlated roughness, the interface profile function $z_0(x)$ is the same for all interfaces and consequently can be factored from the rational expressions, allowing the expectation values to be explicitly calculated. For the cases of uncorrelated and partially correlated roughness, however, the expectation value of the amplitude reflection coefficient is described by the general expression in Eq. (24) below. Here separation of statistically independent components is precluded by the fact that each interface profile appears as an argument in both the numerator and denominator of the expression:

$$\langle \rho \rangle = \left\langle \frac{\mathcal{F}[z_1(x), z_2(x), z_3(x), \ldots, z_{M+1}(x)]}{\mathcal{G}[z_1(x), z_2(x), z_3(x), \ldots, z_{M+1}(x)]} \right\rangle \ . \tag{24}$$

One means of treating this problem is through Taylor expansion of the multilayer amplitude reflection coefficient so that rational arguments may instead be represented as an algebraic sum of terms. At normal incidence, the amplitude reflection coefficient for an interface is determined essentially by the *difference* in refractive indices of the adjacent media [Eq. (12)]. Since the refractive indices for most materials at x-ray wavelengths differ only slightly from one ($n \approx 1 - \delta$ where $\delta \approx 10^{-5}$), the r_j will be on the order of 10^{-5}. Thus, if one expands the multilayer reflectivity in powers of the individual

Fresnel reflection coefficients r_j, it is clear that the expression will be well represented by only the first few terms (we truncate the series at second-order products of the r_j). Although the number of scattering events increases as one considers higher-order reflections in a superlattice, this increase is completely offset by the intensity decrement associated with reflection from an interface, provided the number of interfaces does not approach the order of $1/r_j$. It should be mentioned that by truncating the Taylor expansion at second-order powers of r_j, the description of the reflected intensity reduces to that of the kinematic approximation. Though the true dynamic character can be retained by including higher-order terms, this correction is extremely small for typical multilayers at normal incidence.

The Taylor expansion allows the amplitude reflection and transmission coefficients for the multilayer to be described in terms of statistically independent quantities for which the expectation value can be evaluated. By means of the expansion Eq. (24) can be approximated by the more tractable expression

$$\langle \rho \rangle \approx \mathcal{H}[\langle \mathcal{A}_1[z_1(x)] \rangle, \langle \mathcal{A}_2[z_2(x)] \rangle, \ldots,$$
$$\langle \mathcal{A}_{M+1}[z_{M+1}(x)] \rangle] \ . \tag{25}$$

By substituting expressions (11)–(18) into Eq. (19) and carrying out the expansion, we obtain the following expressions for the amplitude and intensity reflection coefficients of the multilayer:

$$\rho \approx \sum_{j=1}^{M+1} r_j \exp\left[-i\left(s_j + \sum_{k=1}^{j-1} 2a_k\right)\right] \ , \tag{26}$$

$$\rho\rho^* \approx \sum_{j=1}^{M+1} r_j^2 + \sum_{j=2}^{M+1} \sum_{k=1}^{j-1} 2r_j r_k \cos\left[d_k + \sum_{l=k+1}^{j-1} 2a_l + s_j\right] \ . \tag{27}$$

In the above expressions s and d are compact notation for the sum and difference of a and b, respectively,

$$s_j = a_j + b_j = 2\kappa n_{j-1} z_j(x) \ , \tag{28}$$

$$d_j = a_j - b_j = -2\kappa n_j z_j(x) + 2\phi_j \ . \tag{29}$$

B. Caveats of the Taylor expansion

Because of the cosine dependence on the incidence angle θ_i in the general form of the Fresnel reflection coefficients,[40] it is important to note that the Taylor expansion we employ will hold only for a limited range of incidence angles. The truncated expansion applies when $r_j \ll 1$, which is generally fulfilled at x-ray wavelengths for angles of incidence $\theta_i > 40°$. For smaller incidence angles, the r_j tend toward unity, dynamical effects become more important, and a greater number of terms must be retained in the Taylor expansion in order to accurately describe the behavior. For this reason, we assume normal incidence diffraction geometry for the purpose of studying the effects of interfacial roughness in the models shown in Fig. 1. The magnitude of the scattering vector is varied by means of the x-ray wavelength λ rather than the incidence angle θ_i. Since interfacial roughness is

manifested by the dephasing it induces in rays scattered from adjacent points on the interface, it is immaterial whether the severity of the dephasing is varied by means of the wavelength or the incidence angle under the assumptions of the model. Both angle- and wavelength-dispersive techniques are widely applied to the experimental characterization of multilayers.[41,42]

Although strong dynamical scattering cannot be treated under the approximations employed in this model, this shortcoming is ameliorated by the presence of interfacial roughness which partitions intensity away from the specular and into the diffuse field. Roughness induces random phase shifts at the interface thereby hindering constructive interference among multiply scattered rays at the Bragg condition (dynamical diffraction). Even for rough interfaces, however, dynamical effects will become important at sufficiently small q_z, and the implications of this will be discussed in Sec. V B. Finally, by assuming both refractive indices in the multilayer to be real, we have neglected absorption. Though it can easily be included, it is not germane to the goal of these calculations.

IV. APPLICATION TO VARIOUS FORMS OF ROUGHNESS

Using the general expression developed above for the amplitude and intensity reflection coefficients [Eqs. (26) and (27)], we now present expressions for the total, specular, and diffuse reflected intensities for each of the multilayers shown in Fig. 1. This involves substituting the appropriate values of a_j, s_j, and d_j into the general expressions (26) and (27) and calculating the expectation values given by Eqs. (7)–(9). In all cases, the diffracted intensity can be expressed in the following form:

$$R = \sum_{j=1}^{M+1} \alpha(j)r_j^2 + 2 \sum_{j=2}^{M+1} \sum_{k=1}^{j-1} \beta(j,k)r_j r_k \cos\left(\sum_{l=k}^{j-1} 2\phi_l\right).$$

(30)

The only difference between various cases is the prefactors $\alpha(j)$ and $\beta(j,k)$ which we will refer to as the "diffraction coefficients" since they completely characterize the diffracted intensity. This distinction is a natural one since each describes a different physical quantity. The coefficient α describes how the intensity resulting from *incoherent scattering* from individual layers is affected by roughness. Coefficient β, on the other hand, describes how the intensity resulting from *coherent interference* among layers is modified by the roughness. It is important to note that, in general, the coefficients α and β in Eq. (30) are functions of j and k, influenced both by the roughness and correlation of each interface. We reiterate that the r_j and r_k in Eq. (30) correspond to the Fresnel reflection coefficients for the *ideal interface* at normal incidence. We will designate the cases of no roughness, correlated roughness, uncorrelated roughness, and partially correlated roughness by superscripts o, c, u, and p, respectively. The special case of cumulative roughness treated in Sec. IV E will be designated by the superscript q. Once again, the specular, diffuse, and total intensities will be designated by subscripts s, d, and t, re-

spectively. We will use this notation to differentiate the diffraction coefficients. For example, the coefficient for coherent, diffuse scattering from a multilayer with uncorrelated roughness will be designated β_d^u.

A. No roughness

Although the diffraction from an ideal superlattice is well known,[43] we include it to allow comparison with the cases treated subsequently. For a perfectly smooth multilayer the $z_j(x)$ are identically zero, as shown in Fig. 1(a), reducing the quantities $2a_j$, s_j, and d_j to $2\phi_j$, 0, and $2\phi_j$, respectively. By substituting these values into Eqs. (26) and (27) and evaluating expectation values (7)–(9), we obtain the diffraction coefficients given in Table I. As expected, the reflection is entirely specular with no diffuse component. The value for coefficients α^o and β^o of 1 and 0 for the specular and diffuse scattering represent limiting values for these quantities. All subsequent cases involving surface roughness will exhibit coefficients intermediate between these two.

B. Correlated roughness

In this case the interface profile function is nonzero and identical for every interface $[z_j(x)=z_0(x)$ for all $j]$ as shown in Fig. 1(b). The standard deviation for $z_0(x)$ is σ_0. In this case, $2a_j=2\kappa\Delta_j z_0(x)+2\phi_j$, $s_j=2\kappa n_{j-1}z_0(x)$, and $d_j=-2\kappa n_j z_0(x)+2\phi_j$, resulting in the diffraction coefficients given in Table II. Since $\alpha_t^c=\beta_t^c=1$, it is clear that the total intensity scattered from a conformally rough multilayer is identical to that of the ideal multilayer. On the other hand, the specular component exhibits pseudo-Debye-Waller attenuation. The behavior of both quantities is furthermore identical to that of the *single interface* treated in Sec. II F. In Table II we have made the replacement $n_0\equiv1$. Since $\alpha_s^c=\beta_s^c$ and $\alpha_d^c=\beta_d^c$ and all are independent of indices j and k, the specular and diffuse components are merely exponentially modulated replicates of the diffracted intensity of an ideal multilayer. This is illustrated in Figs. 5(a) and 5(b) which show the specular and diffuse intensities from a model multilayer $(20\times[\text{Mo 10 Å/Ni 14 Å}])$ in which $C_j=1.0$ for all j.

C. Uncorrelated roughness

We now impose the condition that the $z_j(x)$ be distinct and statistically uncorrelated, requiring us to use the full expressions in Eqs. (14), (28), and (29) for a_j, s_j, and d_j, respectively. The rms roughness of the jth interface is now given by σ_j. The resulting diffraction coefficients are presented in Table III. We have invoked the approximation $n_j\approx n_0\equiv1$ in the arguments of the exponents in

TABLE I. Diffraction coefficients for no roughness.

o	$\alpha^o(j)$	$\beta^o(j,k)$
t	1	1
s	1	1
d	0	0

TABLE II. Diffraction coefficients for correlated roughness.

c	$\alpha^c(j)$	$\beta^c(j,k)$
t	1	1
s	$\exp(-4\kappa^2\sigma_0^2)$	$\exp(-4\kappa^2\sigma_0^2)$
d	$1-\exp(-4\kappa^2\sigma_0^2)$	$1-\exp(-4\kappa^2\sigma_0^2)$

TABLE III. Diffraction coefficients for uncorrelated roughness.

u	$\alpha^u(j)$	$\beta^u(j,k)$
t	1	$\exp[-2\kappa^2(\sigma_j^2+\sigma_k^2)]$
s	$\exp(-4\kappa^2\sigma_j^2)$	$\exp[-2\kappa^2(\sigma_j^2+\sigma_k^2)]$
d	$1-\exp(-4\kappa^2\sigma_j^2)$	0

Table III. As a result, the Δ_j^2 terms drop out since they are extremely small. This simplification is not extended to the r_j in expression (30), however, since that would suppress scattering altogether. It is interesting to note that in this case the total reflected intensity is less than that of either the ideal or correlated multilayer. This decrease in reflectivity is due solely to the loss of correlation among the layers since only β_t^u is affected. The lost intensity is accounted for by a corresponding increase in the transmitted intensity. Finally, since β_d^u is zero, we see there is no coherency in the diffusely scattered intensity. The lack of correlation between the constituent layers annihilates interference effects leaving only incoherent scattering from the individual rough layers described by α_d^u. This is illustrated in Figs. 5(c) and 5(d) which show the specular and diffuse diffracted intensities from the model multilayer in which $C_j=0$ for all j. The diffuse intensity is featureless while the specular intensity is modulated by the same pseudo-Debye-Waller attenuation as for the case of the correlated multilayer.

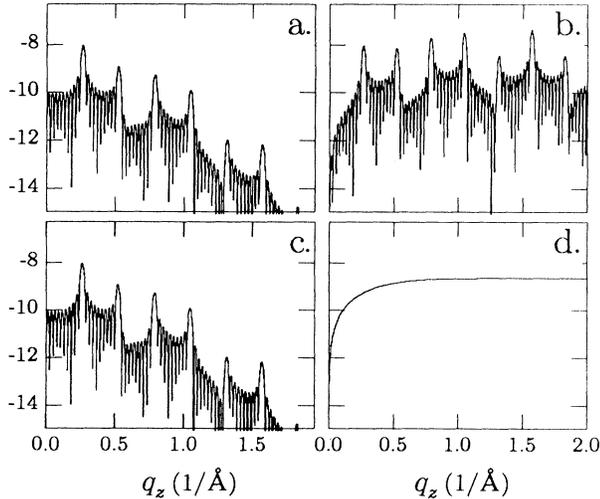If the σ_j are no longer identical but vary with some distribution, the diffraction spectrum can be modified in ways other than pseudo-Debye-Waller attenuation: not only will the intensities be affected, but the *shape* of the spectra will be dramatically influenced. By roughness "distribution" we mean a rms interface roughness that varies from interface to interface within the multilayer $[\sigma_j=\mathscr{F}(j)]$. Figure 6 shows several specular diffraction spectra from the hypothetical Mo/Ni superlattice $(20\times[10\ \text{Å Mo}/14\ \text{Å Ni}])$. In each case the interfacial roughness varies linearly about an average roughness, $\langle\sigma\rangle=2$ Å over a range $\Delta\sigma=0$, 1, and 4 Å, respectively $(\sigma_j=\langle\sigma\rangle+\Delta\sigma[j/(M+1)-\tfrac{1}{2}]$, $M=20)$. Figure 6 shows that with a finite distribution in the σ_j, the peaks broaden in q_z in addition to being attenuated. The broadening becomes more severe as the width of the distribution increases, and the finite size oscillations between Bragg harmonics are obfuscated. Although the correlation coefficients were set to zero in this calculation, similar broadening would occur in the diffuse spectra in instances of nonzero correlation.
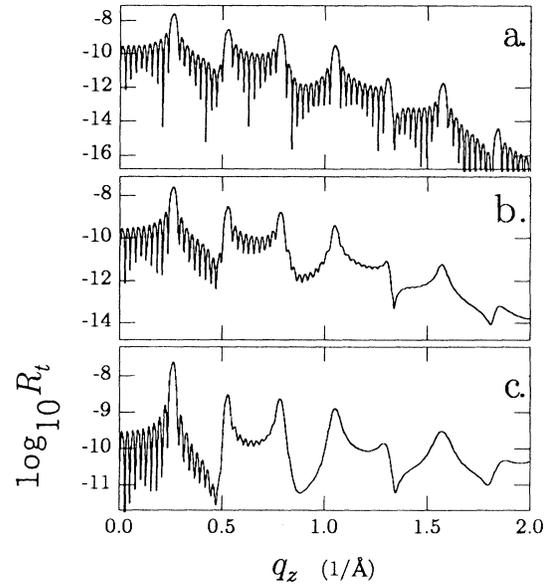

FIG. 5. Figure showing the effect of layer correlation on specular (R_s) and diffuse (R_d) diffracted intensities from an exemplary multilayer, $20\times[10\ \text{Å Mo}/14\ \text{Å Ni}]$: (a) R_s correlated multilayer, (b) R_d correlated multilayer, (c) R_s uncorrelated multilayer, (d) R_d uncorrelated multilayer. Note peaked diffuse scattering for correlated roughness and featureless diffuse background for uncorrelated roughness. Specular scattering from each multilayer is identical.

FIG. 6. Specular intensity from the exemplary multilayer $(20\times[10\ \text{Å Mo}/14\ \text{Å Ni}])$ in which a linear variation in the rms roughness, $\Delta\sigma$, has been imposed on the layers. The average roughness, $\langle\sigma\rangle$, is 2 Å in all cases and the roughness distribution is described by $\sigma_j=\langle\sigma\rangle+\Delta\sigma[j/(M+1)-\tfrac{1}{2}]$, $M=20$. Breadth of the distribution increases from top to bottom; $\Delta\sigma$ is 0, 1, and 4 Å in (a), (b), and (c), respectively. The figure illustrates how *distributions* of the individual layer roughnesses lead to progressive broadening of superlattice peaks and obfuscation of the finite size submaxima. Severity of effect increases with breadth of distribution.

Peak broadening caused by roughness distributions can be understood in terms of Fourier concepts. Roughness distributions endow the superlattice with a locally nonuniform bilayer period Λ which cannot be described exclusively with a harmonic series of Fourier coefficients. On the other hand, a *distribution* of Fourier components around the harmonics can describe the illicit bilayer period and results in the observed peak broadening. We note that the broadening caused by roughness distributions adds to the inherent peak broadening caused by truncation of the structure at a finite number of repeat units. Although we have used linear distribution, it is important to note that broadening will result when there is *any* distribution in the rms interface roughnesses.

D. Partially correlated roughness

As mentioned earlier, partially correlated interfaces can be described by decomposing an interface profile function into a totally correlated component, given by an adjacent interface profile function, and an uncorrelated component representing the intrinsic roughness of the interface. Adjacent interface profile functions can be related by the following recursion relationship:

$$z_{j+1}=\sigma_{j+1}[D_j\hat{\zeta}_{j+1}(x)+C_j\hat{z}_j(x)] . \tag{31}$$

Here $z_j(x)$ is the correlated component while $\zeta_{j+1}(x)$ is the uncorrelated, intrinsic component. The quantities $\hat{z}(x)$ and $\hat{\zeta}(x)$ refer to these functions normalized for a unity standard deviation:

$$\hat{z}(x)=z(x)/\langle z(x)^2\rangle^{1/2} , \tag{32}$$

$$\hat{\zeta}(x)=\zeta(x)/\langle\zeta(x)^2\rangle^{1/2} . \tag{33}$$

It is clear that for partial correlation, each function $z_j(x)$ will be related to each precursor function $z_i(x)$ where $i<j$. By means of the recursion relationship above, however, we can express an interface profile function as a linear combination of the statistically uncorrelated $\hat{\zeta}_j(x)$:

$$z_j(x)=\sigma_j\sum_{l=1}^{j}D_{l-1}\left[\prod_{m=l}^{j-1}C_m\right]\hat{\zeta}_l(x) . \tag{34}$$

In the above equation we define $D_0\equiv 1$ and maintain this definition throughout. Substituting these functions into Eqs. (26) and (27) and evaluating the expectation values given by Eqs. (7)–(9) yields the coefficients given in Table IV. In deriving the expressions in Table IV we have once again neglected Δ_j and Δ_j^2 terms in the exponential arguments through the assumption $n_j\approx n_0\equiv 1$. The coefficient β_t^p is now a function of all layer correlations through the quantity ψ^2 given by

$$\psi^2=\sigma_j^2-2\sigma_j\sigma_k\prod_{l=k}^{j-1}C_l+\sigma_k^2 . \tag{35}$$

The specular diffraction coefficients α_s^p and β_s^p are identical to those of the uncorrelated multilayer indicating that the specularly diffracted intensity is independent of roughness correlations. This is a manifestation of the idea presented in Sec. II D, that the specular intensity results only from the *average* electron density modulation associated with an interface. Because all in-plane roughness effects are averaged in calculating R_s, it is independent of the lateral distributions of the roughness and is therefore not influenced by z correlation. For perfect correlation $(C_j=1, \sigma_j=\sigma_0)$ the above expressions reduce to those in Table II, while for no correlation $(C_j=0)$ they reduce to those in Table III.

Figure 7 shows R_t and R_d from the exemplary multilayer, $20\times[10$ Å Mo/14 Å Ni], under various states of correlation. In each case, the designated correlation coefficients were applied to *each* interface comprising the superlattice. Since a 2-Å roughness was also imposed at each interface, the specular signal exhibits pseudo-Debye-Waller attenuation evinced by the attenuation of the Bragg peaks in the total diffracted intensity. The
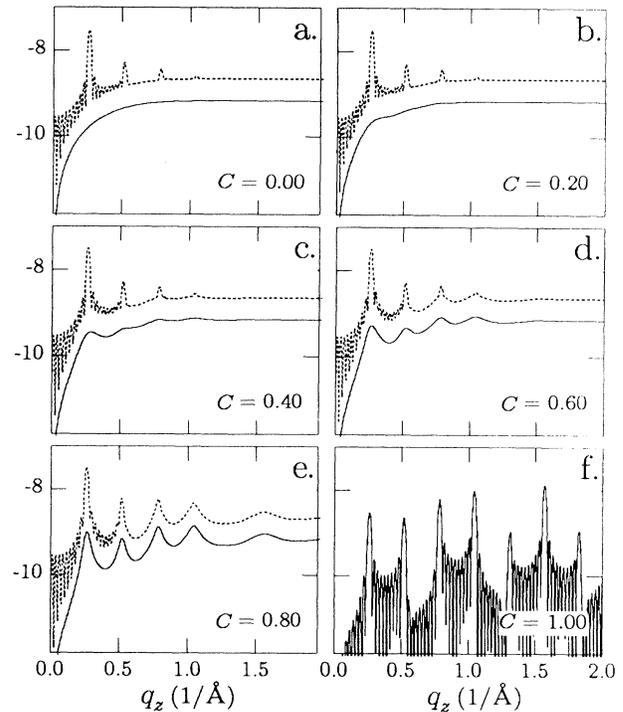

FIG. 7. Composite showing behavior of total diffracted intensity (R_t, dashed line), and the diffuse intensity (R_d, solid line), for the exemplary multilayer ($20\times[10$ Å Mo/14 Å Ni]) under states of correlations indicated. The indicated values of the correlation coefficient were applied to *all* interfaces comprising the superlattice. Diffuse scattering at the Bragg condition increases with correlation. Finite thickness oscillations appear near full correlation $(C=1)$. For clarity, the diffuse intensity has been offset in each of the graphs, and the total intensity has been omitted for the case of full correlation.

TABLE IV. Diffraction coefficients for partially correlated roughness.

p	$\alpha^p(j)$	$\beta^p(j,k)$
t	1	$\exp(-2\kappa^2\psi^2)$
s	$\exp(-4\kappa^2\sigma_j^2)$	$\exp[-2\kappa^2(\sigma_j^2+\sigma_k^2)]$
d	$1-\exp(-4\kappa^2\sigma_j^2)$	$\exp(-2\kappa^2\psi^2)-\exp[-2\kappa^2(\sigma_j^2+\sigma_k^2)]$

specular diffraction signal R_s is omitted in Fig. 7 since it is identical for all states of correlation. The diffuse component R_d is initially featureless for $C = 0$ but begins to show broad peaks at the Bragg conditions as the correlation is increased. As the correlation approaches unity, the diffuse component rapidly sharpens to become an exponentially modulated version of the ideal superlattice diffraction spectra.

E. Cumulative roughness

In the cases treated in Secs. IV A–IV D, a constant correlation was assumed for each interface in the multilayer. This was done so that we might explicitly explore the effect of roughness correlations through the correlation coefficient C. In reality, however, interface correlation is implicitly affected by the nature of the surface on which it is deposited. The propagation of the substrate roughness into the multilayer interfaces, for example, is a recognized and well-studied mechanism by which roughness correlations arise in multilayers.[34,44] In a more general sense, however, roughness correlations can develop in *any* case where interfacial roughness is present. This is because a layer of deposited material must, to some degree, conformally assimilate the shape of the underlying interface profile function. Up to the point at which roughness saturates, these effects are cumulative and their influence thus becomes more pronounced as the number of interfaces increases.

To see this, we envision a nonequilibrium deposition condition in which atoms contributing to the layer "hit and stick" at the surface (gross surface mobility restricted). Figure 8 shows a multilayer in which each 10-Å layer is given an intrinsic rms roughness $\sigma_0 = 1$ Å. In moving from the bottom of the stack upward, it is evident that both the rms roughness and the correlation increase. The latter occurs because the ratio of intrinsic roughness
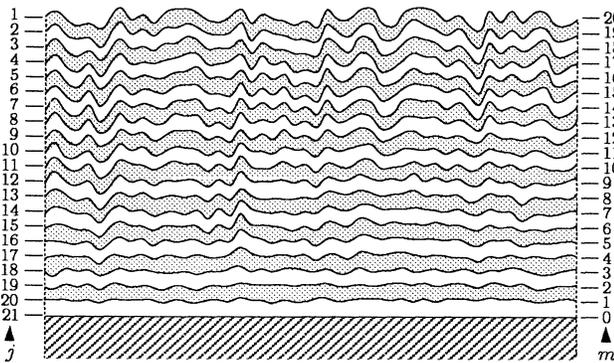
(constant) to cumulative roughness (increasing) decreases as a function of interface position. Both trends are evident in published cross-section transmission electron microscopy (TEM) micrographs of Mo-Si multilayers.[45,46] When this growth mode pertains, the rms roughness at an interface, σ_j, and the correlation coefficient C_j become well-defined functions of their position within the multilayer stack. Figure 9 shows a plot of both quantities as a function of the conjugate layer index $[m \equiv (M + 1) - j]$ for the hypothetical multilayer shown in Fig. 8. The points are described by the following functional forms:

$$\sigma_m = \sqrt{m}\,\sigma_0 , \tag{36}$$

$$C_m = \sqrt{m/(m + 1)} , \tag{37}$$

$$D_m = \sqrt{1/(m + 1)} , \tag{38}$$

where σ_0 in this case represents the rms roughness of the intrinsic, uncorrelated component, $\zeta(x)$, of the interface profile function. It is interesting to note that while the cumulative roughness depends on the intrinsic interface roughness, σ_0, the interfacial correlation is independent of this quantity. This is because correlation is enhanced by cumulative roughness but reduced by intrinsic roughness, *both* of which are governed by σ_0. By substitution of Eqs. (36)–(38) into Eq. (34), we derive the expected result for cumulative roughness, in which an interface profile function is simply the sum of all preceding interface profile functions:

$$z_m(x) = \sum_{l=1}^{m} \zeta_m(x) . \tag{39}$$

If Eq. (39) is substituted into Eqs. (26) and (27) using the substitutions for a_j, b_j, s_j, and d_j given in Eqs. (14), (15), (28), and (29), respectively, the expectation values in Eqs. (7)–(9) can be evaluated to yield the coefficients shown in Table V. The superscript q in this context signifies "cumulative."
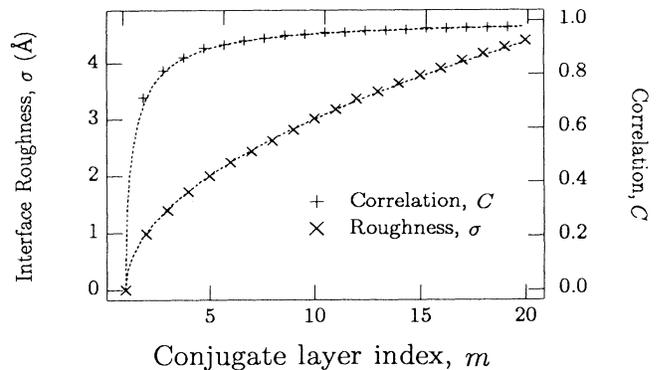

FIG. 8. Schematic showing the evolution of cumulative roughness in an idealized model for multilayer growth $(w_A = w_B = 10$ Å, $\sigma_0 = 1$ Å). The small intrinsic roughness of each layer leads to much larger cumulative roughness toward the top of the superlattice. Layer correlation also visibly increases as the number of layers is increased. The figure is mathematically accurate in that it was generated by spline fitting through a set of 50 interface points each varying with cumulative Gaussian statistics about their mean interface position.

Conjugate layer index, m

FIG. 9. Plot showing behavior of rms interface roughness σ and correlation coefficient C as a function of position within the multilayer. In moving toward the top of the stack σ_m increases as $\sqrt{m}$, while C_m increases as $\sqrt{m/(m + 1)}$. In these expressions m is the conjugate layer index: $m \equiv (M + 1) - j$.

TABLE V. Diffraction coefficients for cumulative roughness.

q	$\alpha^q(j)$	$\beta^q(j,k)$
t	1	$\exp[-2\kappa^2\sigma_0^2(j-k)]$
s	$\exp(-4\kappa^2\sigma_0^2 j)$	$\exp[-2\kappa^2\sigma_0^2(j+k)]$
d	$1-\exp(-4\kappa^2\sigma_0^2 j)$	$\exp[-2\kappa^2\sigma_0^2(j-k)]-\exp[-2\kappa^2\sigma_0^2(j+k)]$

Figures 10(a)–10(c) show R_t, R_s, and R_d for the representative multilayer subject to cumulative roughness effects ($\sigma_0=1.0$ Å). Broadening and attenuation of the specular peaks are evident as a result of the roughness distribution described in Eq. (36). As a result of the evolving correlation within the multilayer, peaked diffuse scattering at the Bragg conditions is also evident in Fig. 10. A noteworthy observation here is that *partial correlation of interface roughness constitutes a second important source of peak broadening in superlattices* which adds to the broadening caused by roughness distributions and truncation effects discussed earlier. In comparing Figs. 10(b) and 10(c) with 10(a) it is clear that in this case, partial correlation is the dominant source of peak broadening, since the roughness leads to predominantly diffuse scattering above $q_z \approx 0.5$ Å^{-1}. Figures 7 and 10 illustrate that partial correlation also affects the finite size oscillations. As the correlation decreases, the oscillations in the diffuse intensity are obfuscated.
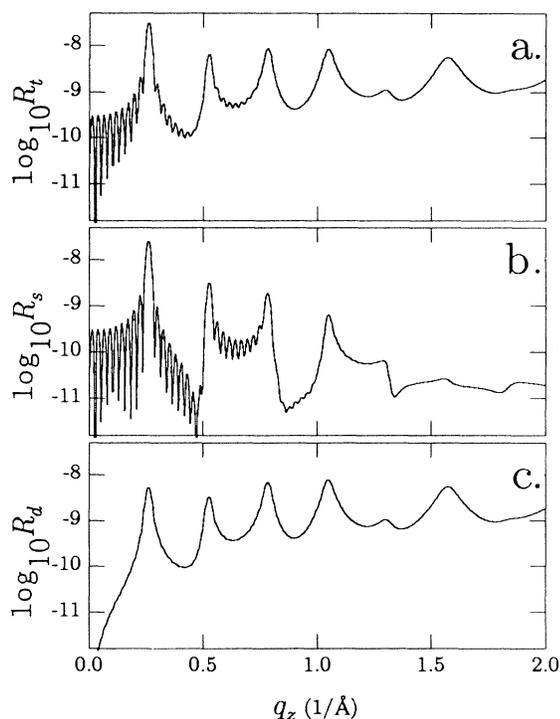

FIG. 10. Total (a), specular (b), and diffuse (c) diffraction spectra for the exemplary multilayer under conditions of cumulative roughness. Intrinsic roughness $\sigma_0=1.0$ Å. Note the severe peak broadening and enhancement of the diffuse scattering near the Bragg conditions. This is a direct result of the roughness and correlation distributions for cumulative roughness shown in Fig. 9.

V. CONCLUSIONS

A. Summary of results

We now summarize the important conclusions from Tables I–V for the multilayer models given in Figs. 1 and 8. For the multilayer without roughness, the incoherent and coherent scattering coefficients (α and β) for specular and diffuse scattering assume the limiting values of 1 and 0, respectively. Upon introducing roughness into the superlattice, these coefficients take on intermediate values as a result of the induced diffuse scattering. The total scattering from the multilayer with correlated roughness is equal to that of a perfect multilayer as a result of the coherent nature of the diffuse scattering. The manner in which the total intensity is partitioned between specular and diffuse components, however, is strongly influenced by the vertical correlation of the roughness. In the absence of correlation more of the incident radiation is transmitted, and the diffracted intensity is reduced from its ideal value. In all cases, the incoherent scattering (coefficient α) is determined exclusively by the roughness of each layer just as for the single surface treated in Sec. II F. While roughness distributions in multilayers induce broadening of the specular Bragg peaks, roughness correlations have no influence on the specular field since it results from the laterally averaged electron density modulation at an interface. Layer correlation affects the diffraction spectrum exclusively through the diffuse term (coefficient β). Partial correlation of interfacial roughness leads to Bragg peaks in the diffuse scattering, although these peaks rapidly broaden as the average correlation of the multilayer deviates significantly from unity.

B. Peaked diffuse scattering

Figure 7 shows that peaked diffuse scattering is a direct consequence of roughness correlations within the multilayer. The analysis clearly shows that correlated roughness is a necessary condition for peaked diffuse scattering. Others have raised the question, however, of whether peaks in the diffuse intensity can result from uncorrelated roughness simply through constructive interference at the Bragg condition, analogous to the intensity enhancement of specular component at these points.[34] In our synchrotron studies of metallic multilayers, we have found that the intensity of a diffuse peak correlates closely with the intensity of the corresponding specular peak, in support of this supposition. We have shown, however, that peaked diffuse scattering *cannot* occur in the absence of roughness correlations. Though we cannot treat strong dynamical scattering due to the truncated Taylor approximation employed here, we maintain that even

strong multiple scattering of the diffusely reflected rays would not lead to features in the diffuse scattering since it is even less likely that third- or fifth-order reflections would interfere coherently than for the first-order reflections treated here. Thus, even under full dynamical treatment, β_d^u would remain zero.

C. Roughness correlation as a consequence of growth

Despite the advanced nature of modern deposition techniques, a thin film will invariably exhibit thickness fluctuations on some level. These effects are generally exacerbated by kinetic or chemical effects such as low surface mobility or high surface energy of the adatom species. For the idealized case of nonequilibrium film growth, we have shown how interfacial roughness might accumulate in multilayers through the collective action of small thickness fluctuations associated with each layer. We have also shown how interface correlation rapidly approaches unity for this idealized growth mode. Two important consequences result from this. First, the specular peaks broaden as a result of the roughness distribution given in Eq. (36). Second, peaked diffuse scattering results simply as a consequence of growth through the naturally occurring correlation given by Eqs. (37) and (38). This explains how significant amounts of peaked diffuse scattering can be observed in multilayers prepared on smooth substrates.[16,33]

Since partial correlation of interfacial roughness is an important source of peak broadening, diffraction models should incorporate a parameter describing this characteristic. This might be something as simple as $\langle C \rangle$, the average correlation in the multilayer: $\langle C \rangle = 1/M(\sum_{j=1}^{M} C_j)$. Whether it is possible to rigorously differentiate roughness distributions from correlation effects using XRD remains to be determined. In cases of moderate correlation and narrow roughness distributions, however, the two effects may be differentiable by inspection as suggested in Fig. 7(d). Here the third and fourth Bragg peaks appear as a superposition of a narrow specular peak over a broad diffuse peak.

D. Implications for modeling of superlattice diffraction

While numerical algorithms typically model the specular intensity, $\langle \rho \rangle \langle \rho^* \rangle$, or total diffracted intensity,

$\langle \rho \rho^* \rangle$, *neither of these quantities is typically measured experimentally* in the regime of low q where the scattered intensity is composed of both specular and diffuse components. In a symmetric scattering geometry $(\theta_i = \theta_o)$, the detector measures the specular intensity plus the component of the diffuse intensity along the specular direction. Some authors have recognized this and account for it by performing nonspecular scans of the diffuse intensity and subtracting this component from the specular data before performing the fitting.[15] A disadvantage of this approach, however, is that in moderately rough multilayers, the diffuse component constitutes the majority of the spectrum, often rich with peaks and features. In such cases, subtracting the diffuse scattering results in a nearly featureless spectrum, thereby discarding valuable information. An alternate, though perhaps less appealing approach to avoid this problem would be to *integrate* the diffuse scattering over the (q_x, q_y) plane and add this intensity to the local origin $(0,0,q_z)$ before fitting to a model for the total diffracted intensity, $\langle \rho \rho^* \rangle$. Since a wide detector slit perpendicular to the scattering plane essentially integrates diffuse intensity along one direction (q_y) in reciprocal space,[32] the total diffuse intensity could be calculated from the area under a rocking curve in q_x, corrected for geometric and refraction effects.[34] Regardless of which technique is ultimately employed, the nonuniform behavior of the specular, diffuse, and total diffracted intensities in the regime of low q underscores the importance of modeling the data against the relevant physical quantity.

[1]Armin Segmuller, I. C. Noyan, and V. S. Speriosu, Prog. Cryst. Growth Charact. **18**, 21 (1989).

[2]B. M. Clemens and J. A. Bain, MRS Bull. **17**, 46 (1992).

[3]H. Homma, K. Y. Yang, and I. K. Schuller, Phys. Rev. B **36**, 9435 (1987).

[4]Chin-An Chang, J. Vac. Sci. Technol. A **9**, 98 (1991).

[5]J. R. Levine, J. B. Cohen, Y. W. Chung, and P. Georgopoulos, J. Appl. Crystallogr. **22**, 528 (1989).

[6]E. Vlieg, A. W. Denier van der Gon, J. F. van der Veen, J. E. Macdonald, and C. Norris, Phys. Rev. Lett. **61**, 2241 (1988).

[7]B. M. Clemens, J. Less Common Met. **140**, 33 (1988).

[8]M. A. Hollanders, B. J. Thijsse, and E. J. Mittenmeijer, Phys.

Rev. B **42**, 5481 (1990).

[9]M. B. Stearns, Phys. Rev. B **38**, 8109 (1988).

[10]W. P. Lowe, T. W. Barbee, Jr., T. H. Geballe, and D. B. McWhan, Phys. Rev. B **24**, 6193 (1981).

[11]E. Spiller, in *Physics, Fabrication and Applications of Multilayered Structures*, edited by P. Dhez and C. Weisbuch (Plenum, New York, 1988).

[12]Eric E. Fullerton, David M. Kelly, J. Guimpel, Ivan K. Schuller, and Y. Bruynseraede, Phys. Rev. Lett. **68**, 859 (1992).

[13]B. M. Clemens and J. G. Gay, Phys. Rev. B **35**, 9337 (1987).

[14]W. Sevenhans, M. Gijs, Y. Bruynseraede, H. Homma, and

Ivan K. Schuller, Phys. Rev. B **34**, 5955 (1986).

[15]D. E. Savage, J. Kleiner, N. Schimke, Y. H. Phang, T. Jankowsky, J. Jacobs, R. Dariotis, and M. G. Lagally, J. Appl. Phys. **69**, 1411 (1991).

[16]B. K. Tanner and J. M. Hudson, IEEE Trans. Magn. **28**, 2736 (1992).

[17]John M. Cowley, *Diffraction Physics* (North-Holland, Amsterdam, 1984).

[18]F. J. Lamelas, H. David He, and Roy Clarke, Phys. Rev. B **43**, 12 296 (1991).

[19]J. P. Locquet, L. Neerinck, L. Stockman, Y. Bruynseraede, and Ivan K. Schuller, Phys. Rev. B **39**, 13 338 (1989).

[20]E. E. Fullerton, I. K. Schuller, H. Vanderstraeten, and Y. Bruynseraede, Phys. Rev. B **45**, 9292 (1991).

[21]W. J. Bartels, J. Hornstra, and D. J. W. Lobeek, Acta Crystallogr. Sect. A **42**, 539 (1986).

[22]J. H. Underwood and T. W. Barbee, Jr., Appl. Opt. **20**, 3027 (1981).

[23]P. Croce, J. Opt. **14**, 213 (1983).

[24]G. V. Rozhnov, J. Opt. **69**, 646 (1989).

[25]J. M. Eastman, in *Physics of Thin Films, Advances in Research and Development,* edited by G. Hass and W. R. Hunter (Academic, New York, 1978), Vol. 10.

[26]J. M. Elson, J. P. Rahn, and J. M. Bennett, Appl. Opt. **19**, 669 (1980).

[27]B. Vidal and P. Vincent, Appl. Opt. **23**, 1794 (1984).

[28]M. Wormington, D. K. Bowen, and B. K. Tanner, in *Structure and Properties of Interfaces in Materials,* edited by W. A. T. Clark, C. L. Briant, and V. Dahmen, MRS Symposia Proceedings No. 238 (Materials Research Society, Pittsburgh, 1992), p. 119.

[29]B. E. Warren, *X-Ray Diffraction* (Addison-Wesley, Reading, MA, 1969).

[30]B. D. Cullity, *Elements of X-Ray Diffraction* (Addison-Wesley, Reading, MA, 1978).

[31]Petr Beckmann and Andre Spizzichino, *The Scattering of Electromagnetic Waves from Rough Surfaces* (MacMillan, New York, 1963).

[32]S. K. Sinha, E. B. Sirota, S. Garhoff, and H. B. Stanley, Phys. Rev. B **38**, 2297 (1988).

[33]A. Bruson, C. Dufour, B. George, M. Vergnat, G. Marchal, and Ph. Mangin, Solid State Commun. **71**, 1045 (1989).

[34]J. B. Kortright, J. Appl. Phys. **70**, 3620 (1991).

[35]D. Chrzan and P. Dutta, J. Appl. Phys. **59**, 1504 (1985).

[36]D. E. Savage, N. Schimke, Y. H. Phang, and M. G. Lagally, J. Appl. Phys. **71**, 3283 (1992).

[37]Po-zen Wong and Alan J. Bray, J. Mod. Opt. **37**, 7751 (1988).

[38]D. G. Stearns, J. Appl. Phys. **65**, 491 (1989).

[39]M. Nieto-Vesperinas, *Scattering and Diffraction in Physical Optics* (Wiley, New York, 1991).

[40]O. S. Heavens, *Optical Properties of Thin Solid Films* (University of Michigan, Ann Arbor, MI, 1989).

[41]D. G. Stearns, R. S. Rosen, and S. P. Vernon, Opt. Lett. **16**, 1283 (1991).

[42]E. Chason, T. M. Mayer, A. Payne, and D. Wu, Appl. Phys. Lett. **60**, 2353 (1990).

[43]M. Born and E. Wolf, *Principles of Optics,* 6th ed. (Pergamon, New York, 1983).

[44]F. E. Christensen, Rev. Phys. Appl. **23**, 1701 (1988).

[45]M. B. Stearns, C. H. Chang, and D. G. Stearns, J. Appl. Phys. **71**, 187 (1992).

[46]D. G. Stearns, R. S. Rosen, and S. P. Vernon, J. Vac. Sci. Technol. A **9**, 2662 (1991).